Event-Driven and Sensorless Photovoltaic System Reconfiguration for Electric Vehicles

Xue Lin, Yanzhi Wang, Massoud Pedram
University of Southern California
Los Angeles, CA, USA
{xuelin, yanzhiwa, pedram}@usc.edu

Jaemin Kim
Seoul National University
Seoul, Korea
jmkim@elpl.snu.ac.kr

Naehyuck Chang
KAIST
Daejeon, Korea
naehyuck@cad4x.kaist.ac.kr

Abstract—This work investigates the problem of increasing the electrical energy generation efficiency of photovoltaic (PV) systems on electrical vehicles (EVs). The PV cell modules of an onboard PV system are mounted on the rooftop, hood, trunk, and door panels of an EV to fully make use of the vehicle surface areas. However, due to the non-uniform distribution and rapid change of solar irradiance, an onboard PV system suffers from significant efficiency degradation. To address this problem, this work borrows the dynamic PV array reconfiguration architecture in previous work with the accommodation of the rapidly changing solar irradiance in the onboard scenario. Most importantly, this work differs from previous work in that (i) we propose an event-driven PV array reconfiguration framework replacing the periodic reconfiguration framework in previous work to reduce the computation and energy overhead of the PV array reconfiguration; (ii) we provide a sensorless (and also event-driven) PV array reconfiguration framework, which further reduces the cost of a vehicular PV system, by proposing a solar irradiance estimation algorithm for obtaining the instantaneous solar irradiance level on each PV cell module. Experimental results demonstrate significant performance enhancement and energy overhead reduction.

I. INTRODUCTION

Electric vehicles (EVs) have again attracted wide attention and interest due to the concerns about increasing oil prices and the need to reduce greenhouse gas emissions [1]. EVs differ from conventional fossil fuel-powered vehicles in that (i) electric motors instead of engines are used for propulsion, (ii) a significant reduction of gas and pollutant emissions, and (iii) electricity consumed by EVs can be generated from a wide range of sources including renewable energy sources.

Thanks to the abundance and easy access of solar energy, photovoltaic (PV) cells provide us a clean and quiet form of electrical energy generation. Moreover, PV cells can be an ideal power source for EVs due to their stability and controllability [2]. The highest solar irradiance during a day is around 1000 W/m^2, the energy conversion efficiency of PV cells is about 30 %, and therefore a PV module with 1 m^2 area can generate a peak power of 300 W. The total horizontal panel area including the rooftop, hood and trunk of a typical passenger vehicle is around 4 - 5 m^2. The electric motor power rating of a modern EV with similar or even higher driving performance than the conventional vehicles is commonly over 100 kW [3]. A passenger vehicle needs high horsepower when accelerating and hill climbing, whereas the moderate horsepower is needed for cruising (e.g., less than 10 kW during city driving.) Therefore, although it may be not practical to realize a fully PV-powered EV with similar driving

performance as a conventional vehicle, an EV with onboard PV electrical energy generation system (PV system) is still beneficial since PV cells can charge the EV battery pack when the EV is running and parking to mitigate the power demand from the grid [2].

To increase the PV electrical power generation capability of a partially PV-powered EV, we should enlarge the onboard PV cell modules by using all possible vehicle surface areas including the rooftop, hood, trunk and door panels. Even though PV cell modules may be mounted on different vehicle surface areas, the *string charger architecture* [4], where PV cell modules are connected in series and a single power converter is employed to control the operating points of the all the PV modules simultaneously, is a practical choice for the onboard PV system taking into account cost considerations and the high voltage of the EV battery pack. Comparing to the *micro charger architecture*, where each PV module has its own power converter for operating point setting, the string charger architecture results in lower cost (since only one power converter is used) and higher overall efficiency (due to the fact that a high output voltage can be achieved by PV modules connected in series to match the battery pack voltage, thereby increasing the efficiency of the power converter) [4].

However, the solar irradiance levels on PV cell modules may be different from each other due to different solar incidence angles. For example, the solar incidence angle on the rooftop or hood PV module is smaller than that on the door PV module at noon, and therefore the solar irradiance level on the rooftop or hood PV module is larger. In addition, the solar irradiance profiles on the driver-side door panel and the passenger-side door panel are virtually opposite to each other determined by the vehicle direction and time of the day. Under the non-uniform distribution of solar irradiance, the output current and thereby the output power of a PV system with the string charger architecture is limited by the PV module with the lowest solar irradiance level [5].

This paper aims at maximizing the output power of a vehicular PV system with the string charger architecture taking into account the non-uniform distribution of solar irradiance levels on different vehicle surface areas. This work is based on the dynamic PV array reconfiguration architecture from previous work [5], [6] with the accommodation of the rapidly changing solar irradiance in the onboard scenario. Most importantly, this work differs from previous dynamic PV array reconfiguration work [5], [6] in that (i) first, we propose an event-driven PV array reconfiguration framework replacing the periodic reconfiguration framework in previous work [5], [6] to reduce the computation and energy overhead of the PV
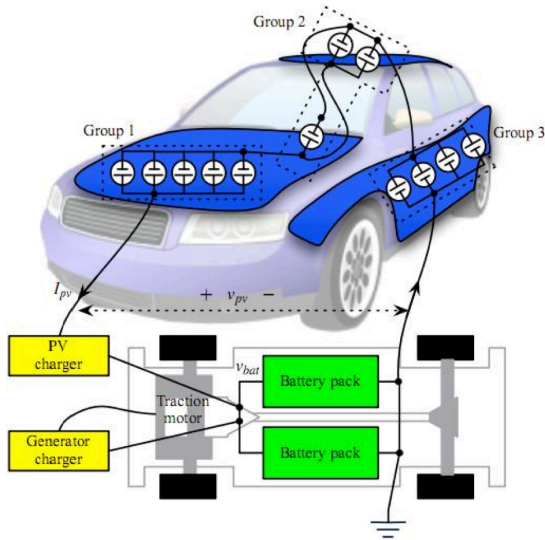
Fig. 1. System diagram of a PV system on the electric vehicle.

Fig. 2. I-V and P-V output characteristics of a PV cell.

Fig. 3. PV array reconfiguration structure.

array reconfiguration; (ii) second, we provide a sensorless (and also event-driven) PV array reconfiguration framework, which further reduces the cost of a vehicular PV system, by proposing a solar irradiance estimation algorithm for estimating the instantaneous solar irradiance level on each PV cell module. The solar irradiance estimation algorithm is supported by the dynamic PV array reconfiguration architecture by only activating PV cells in one PV module while bypassing all others. We implement a high-speed, high-voltage PV array reconfiguration switch network with IGBTs (insulated-gate bipolar transistors) and the CAN (controller area network.) Furthermore, we implement a solar irradiance sensor network for acquiring benchmark solar irradiance profiles on vehicle panels to evaluate our proposed PV array reconfiguration frameworks. Experimental results demonstrate that the event-driven framework achieves up to 2.85X performance enhancement and the sensorless framework achieves up to 2.77X performance enhancement compared with the baseline.

II. ONBOARD PV SYSTEM

Fig. 1 shows the system diagram of an onboard PV system. PV cell modules mounted on the rooftop, hood, trunk and door panels constitute the whole PV array. Depending on the available area on each vehicle panel, PV modules may consist of different numbers of PV cells. As shown in Fig. 1, a charger (i.e., power converter) connects the whole PV array with the EV battery pack for regulating the operating point of the PV array. This is the string charger architecture [4], where PV modules in series share a single power converter. The power modeling of a charger was proposed in [8]. Generally speaking, the energy efficiency of a power converter is high when its input and output voltages are close to each other. Therefore, due to the high voltage of the vehicle battery pack [9], the string charger architecture has the potential for achieving high overall system efficiency.

A. PV Cell Modeling

The whole PV array consists of multiple identical PV cells. We use the method in [10] to extract PV cell modeling. Fig. 2 shows the current-voltage (I-V) and power-voltage (P-V) output characteristics of a PV cell under different solar
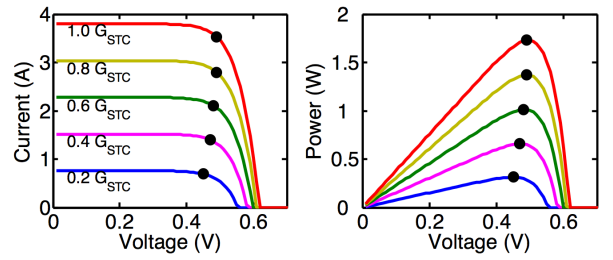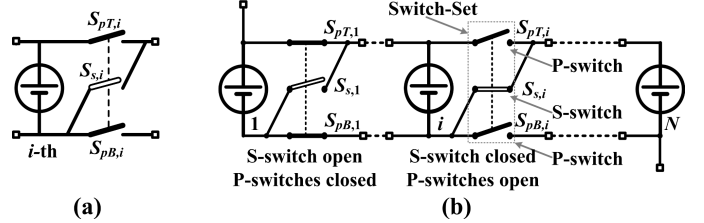
irradiance levels, where $G_{STC} = 1000$ W/m^2 stands for the solar irradiance level under standard test condition. On the PV cell I-V output curves, the solid black dots represent the *maximum power points (MPPs)* of a PV cell, which correspond to the peak power points on the P-V output curves. The maximum output power of a PV cell increases as solar irradiance increases. A charger (or power converter) can regulate the operating point of the PV array by controlling the output current of the charger. Generally, the maximum power point tracking (MPPT) and maximum power transfer tracking (MPTT) techniques are employed in the charger controller to track maximum output power under changing solar irradiance.

B. PV Reconfiguration Structure

A conventional PV array has a fixed $n \times m$ configuration, where n PV cells are series-connected and m PV cells are parallel-connected. When the PV array receives uniform solar irradiance, the PV cells can be set to operate at their MPPs simultaneously and therefore the PV array achieves the maximum output power. However, in reality, especially for an onboard PV system, PV modules mounted on different vehicle panels receive different solar irradiance levels, which also keep changing during driving. This non-uniform distribution of solar irradiance on a PV array results in significant output power degradation due to the fact that PV cells cannot operate at their MPPs simultaneously.

The dynamic PV array reconfiguration method [5], [6] was proposed to address the output power degradation problem under the non-uniform distribution of solar irradiance. The PV reconfiguration method has the potential to make PV cells operate at their MPPs simultaneously even under non-uniform solar irradiance. Fig. 3 presents the structure of a reconfigurable PV array [6] with a total number of N PV cells. Please note that in an onboard PV system, PV cells in the reconfigurable PV array come from all PV modules mounted on the rooftop, hood, trunk, and door panels. Fig. 3 (b) represents the electric connection of PV cells instead of their physical locations.

As shown in Fig. 3 (a), each i-th PV cell is integrated with three solid-state switches: a top parallel switch $S_{pT,i}$,

a bottom parallel switch $S_{pB,i}$, and a series switch $S_{s,i}$. The reconfigurable PV array can change its configuration by controlling the ON/OFF states of the switches. The two parallel switches of a PV cell are always in the same state, and the series switch of a PV cell is in the opposite state of its parallel switches. The parallel switches connect PV cells in parallel forming *PV cell groups*, whereas the series switches connect PV cell groups in series forming a PV array configuration. Now we provide the formal definition of the configuration of a reconfigurable PV array. Consider a reconfigurable PV array with N PV cells, it can have an arbitrary number (less than or equal to N) of PV cell groups. The number of parallel-connected PV cells in the j-th PV cell group (i.e., $r_j > 0$) should satisfy:

$$\Sigma_{j=1}^{g} r_j = N, \qquad (1)$$

where g is the number of PV cell groups. We define the configuration as $\mathcal{C}(g; r_1, r_2, ..., r_g)$. The configuration can be viewed as a partitioning of the PV cell index set $\boldsymbol{A} = \{1, 2, ..., N\}$. The partitioning is denoted by subsets $\boldsymbol{B}_1$, $\boldsymbol{B}_2$, ..., and $\boldsymbol{B}_g$ of $\boldsymbol{A}$, which correspond to the g PV cell groups comprised of r_1, r_2, ..., and r_g PV cells, respectively. The subsets satisfy

$$\cup_{j=1}^{g} \boldsymbol{B}_j = \boldsymbol{A}, \qquad (2)$$

and

$$\boldsymbol{B}_j \cap \boldsymbol{B}_k = \emptyset, \forall j, k \in \{1, 2, ..., g\}, j \neq k. \qquad (3)$$

Due to the structure characteristics of the reconfigurable PV array, we also have $i_1 < i_2$ for $\forall i_1 \in \boldsymbol{B}_j$ and $\forall i_2 \in \boldsymbol{B}_k$ satisfying $1 \leq j < k \leq g$. A partitioning satisfying the above properties is called an *alphabetical partitioning*.

C. PV Array Reconfiguration Algorithm

A polynomial-time PV array reconfiguration algorithm was proposed in [6], which finds the optimal PV array configuration given the solar irradiance levels on all the PV cells to maximize the PV system output power. The PV array reconfiguration algorithm is comprised of an outer loop to find the optimal number of PV cell groups in the PV array and a kernel algorithm to determine the optimal configuration based on the optimal number of PV cell groups given by the outer loop. This reconfiguration algorithm (i) should be executed frequently to keep the PV array configuration updated under changing solar irradiance; and (ii) needs the knowledge of solar irradiance levels on all the PV cells as the input, or at least solar irradiance levels on the five panels, i.e., rooftop, hood, trunk, right door and left door panels, for an onboard PV system if we assume the solar irradiance is uniform on each vehicle panel. It is straightforward to acquire such solar irradiance information via sensors if five sensors are attached to the five panels, respectively. However, in the sensorless case in which the system is not equipped with solar sensors, we need additional steps to estimate the solar irradiance levels on the five panels, as shown in Section VI. This reconfiguration algorithm will serve as a basis for our event-driven and sensorless PV array reconfiguration frameworks in the present work.

III. OVERVIEW OF THE TWO PROPOSED PV RECONFIGURATION FRAMEWORKS

The most straightforward reconfiguration method, i.e., periodic reconfiguration, was used in [6], [7] in order to keep the configuration of the PV array updated periodically under rapidly changing solar irradiance. The reconfiguration period

is a critical design parameter. A large reconfiguration period may not be able to capture the fast change in solar irradiance levels, whereas a small reconfiguration period will induce high timing and energy overheads and may eventually degrade the PV system performance. The optimal reconfiguration period may be quite different for various driving scenarios (i.e., city driving vs freeway driving.) Therefore, in the present work we propose an event-driven PV array reconfiguration framework, in which the PV array reconfiguration algorithm is triggered only if there is noticeable change in the solar irradiance levels. In this way, timing and energy overheads of PV reconfiguration can be largely reduced.

By a thorough examination of the reconfigurable PV array structure, we found that it has the potential for achieving more flexible PV array configurations, in which part of the PV cells are active and the rest of the PV cells can be bypassed. Based on this observation, we provide a solar irradiance estimation algorithm to estimate the instantaneous solar irradiance level on each PV cell module. Therefore, we go one step further to propose the sensorless PV array reconfiguration framework that reduces the capital cost of an onboard PV system due to the sensor node network. The sensorless framework is also event-driven to decrease the timing and energy overheads.

Next we will first describe the PV reconfiguration hardware design, including the IGBT (insulated-gate bipolar transistor)-based reconfiguration switch network, the solar irradiance sensor network to acquire instantaneous solar irradiance levels and benchmark solar irradiance profiles, as well as a thorough overhead analysis of various components in the reconfiguration system. Finally we will describe the event-driven (and sensor-based) reconfiguration framework and the sensorless (and event-driven) reconfiguration framework, respectively.

IV. PV RECONFIGURATION HARDWARE DESIGN
A. IGBT-Based Reconfiguration Switch Network

In the onboard scenario, the rapid change of vehicle driving direction results in fast changing of solar irradiance levels on PV modules, which demands fast PV array reconfiguration within a few milliseconds. In addition, high-voltage or high-current gate control is required for switches in the reconfigurable vehicular PV array. Therefore, we implement an IGBT (insulated-gate bipolar transistor)-based reconfiguration switch network to meet the above mentioned requirements.

We carefully select commercial IGBTs and gate drivers for switches in the reconfigurable PV array. The selected IGBT IXXK200N65B4 can handle voltage and current ratings of 650 V and 370 A, respectively, which are sufficient ratings for vehicular PV arrays. We select gate driver MC33153 that has a small propagation delay of few hundreds nanoseconds to control the IGBTs. The photo-coupler isolation is used between the high-voltage IGBT side and the controller logic side to prevent damage due to power surge. The stability of the IGBT and gate driver selections has been verified using square-wave input voltage on the gate driver.

We implement a communication system using the controller area network (CAN). The CAN employs a bus structure for the integration with sensor nodes (if sensors are incorporated). We carefully select ADM3053 as the isolated CAN physical layer transceiver with LM3S2965 as the control processor, which supports hardware layers of CAN communications. 1 Mbps communication speed in transmission makes the transmission delay below 1 ms.

B. Solar Irradiance Sensor Network

In order to (i) acquire instantaneous solar irradiance levels on PV modules in the event-driven (with sensors) PV array reconfiguration framework and (ii) acquire benchmark solar irradiance profiles on vehicle panels for evaluating the proposed PV reconfiguration frameworks, we build a Zigbee-based solar irradiance sensor node network and a logger program.

Zigbee is a wireless network protocol to create personal networks, which is commonly used for low power and low data-rate applications. We use dual AAA-size batteries to supply power for each sensor node without DC-DC converter. Each sensor node is integrated with a Zigbee transceiver module, which automatically reads value from the sensor with its internal ADC and sends it to a receiving node every 50 ms with 250 kbit/s data transmission speed. A specially designed logger program collects sensor data from the receiving node with vehicle speed and location information from GPS. We install magnets to each corner of a sensor node to stick the sensor node to vehicle surface easily and firmly. We attach five sensor nodes at the rooftop, hood, trunk, left side and right side of a vehicle to measure benchmark solar irradiance profiles G_{roof}, G_{hood}, G_{trunk}, G_{left}, and G_{right}, respectively.

C. Overhead Analysis

To justify the proposed PV array reconfiguration frameworks, we need a thorough analysis of both timing overhead and energy overhead of various components/processes in the reconfiguration system:

1) Sensing: With the above mentioned sensor network, each sensor node senses and converts the solar irradiance data every 50 ms, which is the sensing period. Based on the ADC setup, the sensing delay T_{sense} is less than 10 µs.

2) Transmission: The transmission delay T_{trans} of the sensor network is no more than 1 ms using CAN transmission protocol.

3) Computation: For a moderate-scale PV array with 60 PV cells, it only takes 3 - 4 ms to calculate the optimal configuration on a 3.0 GHz desktop computer. The computation delay T_{com} should take less than 10 ms on a typical ARM-based embedded processor (as the reconfiguration controller) [11].

4) Reconfiguration: Our experiments show that the gate drivers and IGBTs can reconfigure within 10 µs with only a little distortion of waveform. Therefore, 1 ms should be a safe estimation of the reconfiguration delay T_{recon}.

5) MPPT or MPTT control: The MPPT or MPTT technique used for tracking maximum output power of the PV array or the PV system has a control delay $T_{control}$ less than 2.5 ms if the perturb & observe-based control is employed.

As for the energy overhead, the vehicular PV system has zero output power during reconfiguration (i.e., changing the ON/OFF states of switches) and has sub-optimal output power during MPPT or MPTT control.

V. EVENT-DRIVEN PV ARRAY RECONFIGURATION

In this section, we propose the event-driven PV array reconfiguration framework to overcome the difficulty in determining the optimal reconfiguration period. Inspired by the event-driven power modeling and power management techniques [14], [15],

the PV array reconfiguration is triggered only by the *event* to avoid unnecessary timing and energy overheads involved in the reconfiguration. For example, if the solar irradiance is stable and the driving direction does not change, there is no reconfiguration performed in our event-driven framework (and there is also no reconfiguration required). Once the PV array reconfiguration is triggered, the reconfiguration controller uses the latest sensed solar irradiance levels on the five panels to calculate the optimal configuration (using the PV array reconfiguration algorithm discussed in Section II-C), and subsequently perform reconfiguration and MPPT/MPTT control.

The PV array should reconfigure with the solar irradiance changes, and therefore we use the change of the solar irradiance sensor readout as the event, i.e., only if the readout of any sensor has a change larger than ΔG, the PV array reconfiguration will be triggered. Upon triggered by an event, the PV reconfiguration will take about 13.5 ms, i.e., the summation of the computation delay, reconfiguration delay, and MPPT or MPTT control delay as listed in Section IV-C, which is the timing overhead. The PV system will have zero output power during reconfiguration and MPPT/MPTT control (please note that this is a conservative estimation).

We use the adaptive learning method to derive the optimal ΔG value in an online manner [12]. We maintain multiple candidate ΔG values, and choose one with the currently highest performance. After a period of time, we evaluate all the candidate ΔG values and update their performance using an exponential weighting function [13]. Then, the candidate value with the highest performance is chosen as the current ΔG. Please note that to avoid over-frequent reconfiguration, we limit the maximum reconfiguration frequency by 10 Hz (1/100 ms). Please refer to Algorithm 1 for details.

Algorithm 1 Adaptive Learning-Based Event-Driven PV Array Reconfiguration

---

1: This algorithm is performed at a learning period of length D. Please note that this learning period is in the order of minutes or even hours and is much longer than typical time intervals between reconfigurations (in the order of 100ms to seconds.)
2: $\Delta G \leftarrow$ the optimal one from the candidates with the highest performance.
3: Maintain $G_{roof}(t_{pre})$, $G_{hood}(t_{pre})$, $G_{trunk}(t_{pre})$, $G_{left}(t_{pre})$, and $G_{right}(t_{pre})$ values.
4: **while** in this learning period **do**
5:     Monitoring solar irradiance levels on the five vehicle panels: $G_{roof}(t)$, $G_{hood}(t)$, $G_{trunk}(t)$, $G_{left}(t)$, and $G_{right}(t)$.
6:     $\Delta G_{roof} = |G_{roof}(t) - G_{roof}(t_{pre})|$;
7:     $\Delta G_{hood} = |G_{hood}(t) - G_{hood}(t_{pre})|$; $\Delta G_{trunk} = ...$; ...
8:     **if** $max\{\Delta G_{roof}, \Delta G_{hood}, \Delta G_{trunk}, \Delta G_{left}, \Delta G_{right}\} > \Delta G$ **then**
9:         Execute the PV array reconfiguration algorithm in [6] and perform reconfiguration.
10:         $G_{roof}(t_{pre}) \leftarrow G_{roof}(t)$; $G_{hood}(t_{pre}) \leftarrow G_{hood}(t)$;
11:         $G_{trunk}(t_{pre}) \leftarrow G_{trunk}(t)$; ...
12:     **end if**
13: **end while**
14: Evaluate all the candidate ΔG values and update their performance using an exponential weighting function.
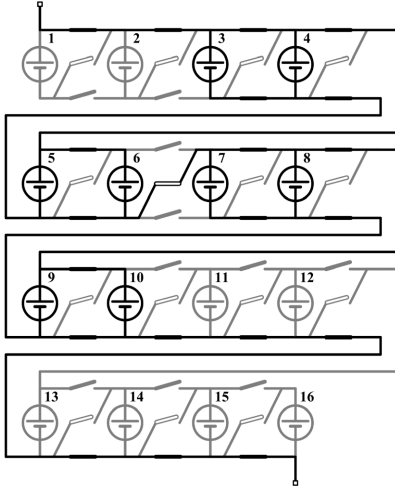

Fig. 4. An illustration of the solar irradiance estimation algorithm.

VI. Sensorless PV Array Reconfiguration

In this section, we propose the sensorless PV array reconfiguration framework to further reduce the capital cost of an onboard PV system due to the sensor node network (please note that the elimination of solar sensors will help make the vehicle surfaces smooth.) Due to the absence of solar sensors, we propose a solar irradiance estimation algorithm to estimate the instantaneous solar irradiance level on each PV module. According to the PV cell characteristics, the MPP power of a PV cell (or PV module) is proportional to the solar irradiance level on it, and therefore we can infer the solar irradiance level on a PV cell (or PV module) from its measured MPP power. Based on the structural characteristics of the reconfigurable PV array, we can form an $n \times m$ configuration with PV cells from one PV module mounted on one vehicle panel, whereas the rest of the PV cells can be bypassed. Then we perform MPPT control on the $n \times m$ configuration to measure the MPP power thereby inferring the solar irradiance level on this PV module.

Fig. 4 shows how to achieve a 2×4 configuration out of the 16-cell reconfigurable PV array. In this 2×4 configuration, only PV cells 3 - 10 are active and the rest of the PV cells are bypassed. Suppose PV cells 3 - 10 belong to the PV module mounted on the hood panel, and we assume the solar irradiance is uniform on this panel. If we measure the MPP power of these PV cells using MPPT control, the solar irradiance level on these PV cells can be inferred. Since there are only five PV modules (each of which is mounted on a vehicle panel) in the vehicular PV system, we can estimate the solar irradiance levels on these PV modules after five times of reconfiguration and MPPT control. Therefore, the timing overhead of one reconfiguration in the sensorless PV reconfiguration framework should be calculated as

$$5 \cdot (T_{recon} + T_{control}) + T_{com} + T_{recon} + T_{control}, \quad (4)$$

which is 31 ms according to the values of delay components listed in Section IV-C. The PV system will have zero output power during the whole 31 ms (please note that this is a conservative estimation).

In the sensorless PV array reconfiguration framework, the timing and energy overheads are larger due to the solar irradiance estimation procedure. Therefore, it is beneficial to

make the sensorless framework also event-driven in order to limit the total number of reconfigurations and thereby total timing and energy overheads. Different from Section V that uses the change of sensor readout as the event to trigger PV reconfiguration, the sensorless PV array reconfiguration framework uses the change of system output power (i.e., the output current of the charger) as the event because only the PV system output power is available to be measured at runtime in the sensorless setup. The adaptive learning method is also employed to derive the optimal ΔP value in an online manner. Details are illustrated in Algorithm 2.

Algorithm 2 Adaptive Learning-Based Sensorless PV Array Reconfiguration

---

1: This algorithm is performed at a learning period of length D.
2: $\Delta P \leftarrow$ the optimal one from the candidates with the highest performance.
3: Maintain $P_{out}(t_{pre})$ corresponding to the PV system output power after the previous reconfiguration.
4: **while** in this learning period **do**
5:   Monitoring the PV system output power $P_{out}(t)$.
6:   **if** $|P_{out}(t) - P_{out}(t_{pre})| > \Delta P$ **then**
7:     **for** each PV cell module **do**
8:       Activate the PV cells in the module while disabling the rest PV cells in the array.
9:       Perform MPPT control to obtain the MPP and estimate the solar irradiance level on this PV module.
10:    **end for**
11:    Execute the PV array reconfiguration algorithm in [6] and perform reconfiguration.
12:    Measure the current $P_{out}(t)$ and set $P_{out}(t_{pre}) \leftarrow P_{out}(t)$;
13:   **end if**
14:   Evaluate all the candidate ΔP values and update their performance using an exponential weighting function.
15: **end while**

VII. Experimental Results

In this section, we justify the two proposed frameworks using the measured solar irradiance traces from the Zigbee-based solar irradiance sensor node network and the logger program. We drive a vehicle along six paths to collect Traces 1 - 6: Incheon airport, Ontario to Riverside, west Los Angeles to Indio, west Los Angeles to Carson, west Los Angeles to Riverside, and Riverside. Each trace consists of five solar irradiance profiles on the rooftop, hood, trunk, left door and right door, respectively.

We measure a mid-size family sedan Renault-Samsung NEW-SM5 car and observe the following area parameters: roof: 1.99 m^2 (1.274 m by 1.565 m); hood: 1.6 m^2 (1.024 m by 1.565 m), trunk: 0.63 m^2 (0.400 m by 1.565 m), left and right door: 1.7 m^2 each (0.616 m by 2.760 m). These values are the available installation area for each PV module. We assume fixed-size PV cells with 0.15 m^2 area each, 20 V MPP voltage, and 2.25 A MPP current at $G = 1000$ W/m^2. We assume 200 V terminal voltage of the EV battery pack. We consider a realistic PV charger model with efficiency variations [8]. We also consider a baseline setup, which has the same PV modules as in the proposed frameworks but without PV reconfiguration.

Table I compares the average system output power values from the event-driven (and sensor-based) framework, the sensorless framework, and the baseline under all the

	Trace 1	Trace 2	Trace 3	Trace 4	Trace 5	Trace 6
Event-Driven	1055.1	524.1	849.9	808.0	475.9	1037.6
Sensorless	1034.6	514.9	822.4	760.6	461.2	1004.5
Baseline	687.8	329.1	535.9	479.7	166.7	576.8
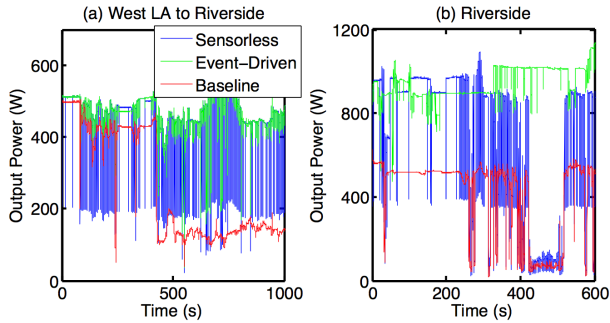
Fig. 5.   Output power profiles of the event-driven, sensorless, and baseline frameworks.

Fig. 6.   Energy overhead and average output power comparisons of periodic and event-driven frameworks.

six driving traces. Both the event-driven framework and the sensorless framework outperform the baseline significantly, demonstrating the effectiveness of the even-driven PV array reconfiguration and the solar irradiance estimation algorithm. Specifically, comparing with the baseline, the event-driven framework achieves up to 2.85X performance enhancement, and the sensorless framework achieves up to 2.77X performance enhancement.

From the output power values in Table I, we can also observe that the even-driven (and sensor-based) framework achieves higher average system output power than the sensorless framework, which is due to the following reasons: (i) the sensorless framework has higher timing and energy overheads due to the solar irradiance estimation process, and (ii) in the sensorless framework, we can only use the system output power change rather than the solar irradiance change as the event to trigger reconfiguration.

Fig. 5 shows the output power profiles of the event-driven framework, the sensorless framework, and the baseline under (a) Trace 5 and (b) Trace 6, which again demonstrates that the proposed two frameworks outperform the baseline and the event-driven framework achieves slightly higher output power than the sensorless framework. Please note that on the output power profiles of the event-driven and sensorless frameworks, there are some sudden power drops, which are the energy overhead of the PV reconfiguration. The power values in Fig. 5 are actually the average output power in a 50 ms time window. The amplitude of power drop in the sensorless framework is larger than that in the event-driven framework due to the energy overhead involved in the solar irradiance estimation process. However, the overall performance of the sensorless framework is quite close to the event-driven (and sensor-based) framework as shown in Table I due to the relatively infrequent reconfigurations.

Fig. 6 compares the reconfiguration energy overhead and average output power of the event-driven framework and the periodic framework under Traces 1 - 4. We use reconfiguration periods 0.1 s, 0.2 s and 0.5 s in the periodic framework. The reconfiguration period of 0.5 s is the optimal one in terms of the overall system performance. We can observe that the event-driven framework reduces the energy overhead by around 50 % compared to reconfiguration with a period of 0.5 s. The
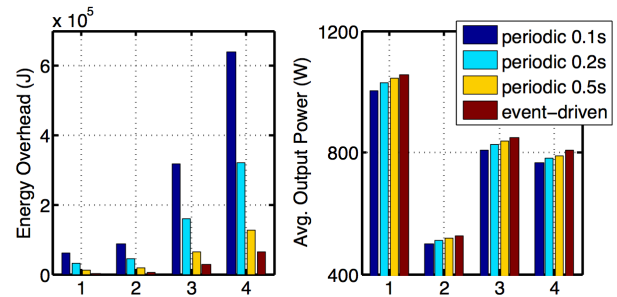
energy overhead reduction implies fewer reconfiguration times and therefore prolonged system lifespan. Compared to the reconfiguration with a period of 0.1 s, the energy overhead of the event-driven framework is even negligible. Furthermore, the average output power of the event-driven framework is the highest.

VIII.   CONCLUSION

Due to the non-uniform distribution and rapid change of solar irradiance, an onboard PV system suffers from significant efficiency degradation. This work borrows the dynamic PV array reconfiguration architecture in previous work with the accommodation of the rapidly changing solar irradiance in the onboard scenario. This work differs from previous work in that (i) we propose an event-driven PV array reconfiguration framework to reduce the computation and energy overhead; (ii) we provide a sensorless PV array reconfiguration framework to further reduce the cost of a vehicular PV system.

REFERENCES

[1]   S. Park, Y. Kim, and N. Chang, "Hybrid energy storage systems and battery management for electric vehicles," *Proc. DAC*, 2013.

[2]   Solar powered vehicles: http://www.designboom.com/contemporary/solarpoweredvehicles.html.

[3]   A. Affanni, A. Bellini, G. Franceschini, et al., "Battery choice and management for new-generation electric vehicles," *IEEE TIE*, Oct. 2005.

[4]   W. Xiao, N. Ozog, and W. G. Dunford, "Topology study of photovoltaic interface for maximum power point tracking," *IEEE TIE*, Jun. 2007.

[5]   Y. Wang, X. Lin, Y. Kim, et al., "Enhancing efficiency and robustness of a photovoltaic power system under partial shading," *Proc. ISQED*, 2012.

[6]   X. Lin, et al., "Near-optimal, dynamic module reconfiguration in a photovoltaic system to combat partial shading effects," *Proc. DAC*, 2012.

[7]   J. Kim, Y. Wang, et al., "Fast photovoltaic array reconfiguration for partial solar powered vehicles," *Proc. ISLPED*, 2014.

[8]   Y. Wang, Y. Kim, et al., "Charge migration efficiency optimization in hybrid electrical energy storage (HEES) systems," *Proc. ISLPED*, 2011.

[9]   S. J. Moura, H. K. Fathy, D. S. Callaway, et al., "A stochastic optimal control approach for power management in plug-in hybrid eletric vehicles," *IEEE TCST*, May 2011.

[10]   W. Lee, Y. Kim, Y. Wang, et al., "Versatile high-fidelity photovoltaic module emulation system," *Proc. ISLPED*, 2011.

[11]   *Samsung Exynos 4 Dual 45nm (Exynos 4210) Microprocessor, 2012.*

[12]   C. M. Bishop, *Pattern Recognition and Machine Learning*. Springer, 2007.

[13]   C. Hwang and A. C. Wu, "A predictive system shutdown method for energy saving of event-driven computation," *ACM Trans. Design Automation of Electronic Systems*, Apr. 2000.

[14]   T. Simunic, L. Benini, P. Glynn, et al., "Event-driven power management," *IEEE TCAD*, Jul. 2001.

[15]   C. Yoon, D. Kim, W. Jung, et al., "Appscope: application energy metering framework for android smartphones using kernel activity monitoring," in *USENIX ATC*, 2012.